

Influence of $Zr_{50}Cu_{50}$ thin film metallic glass as buffer layer on the structural and optoelectrical properties of AZO films*

Bao-Qing Zhang(张宝庆)¹, Gao-Peng Liu(刘高鹏)¹, Hai-Tao Zong(宗海涛)^{2,†}, Li-Ge Fu(付丽歌)², Zhi-Fei Wei(魏志飞)¹, Xiao-Wei Yang(杨晓炜)¹, and Guo-Hua Cao(曹国华)^{2,‡}

¹School of Materials Science and Engineering, Henan Polytechnic University, Jiaozuo 454000, China

²School of Physics and Electronic Information Engineering, Henan Polytechnic University, Jiaozuo 454000, China

(Received 29 December 2019; revised manuscript received 10 January 2020; accepted manuscript online 16 January 2020)

Aluminum-doped ZnO (AZO) thin films with thin film metallic glass of $Zr_{50}Cu_{50}$ as buffer are prepared on glass substrates by the pulsed laser deposition. The influence of buffer thickness and substrate temperature on structural, optical, and electrical properties of AZO thin film are investigated. Increasing the thickness of buffer layer and substrate temperature can both promote the transformation of AZO from amorphous to crystalline structure, while they show (100) and (002) unique preferential orientations, respectively. After inserting $Zr_{50}Cu_{50}$ layer between the glass substrate and AZO film, the sheet resistance and visible transmittance decrease, but the infrared transmittance increases. With substrate temperature increasing from 25 °C to 520 °C, the sheet resistance of AZO(100 nm)/ $Zr_{50}Cu_{50}$ (4 nm) film first increases and then decreases, and the infrared transmittance is improved. The AZO(100 nm)/ $Zr_{50}Cu_{50}$ (4 nm) film deposited at a substrate temperature of 360 °C exhibits a low sheet resistance of 26.7 Ω/\square , high transmittance of 82.1% in the visible light region, 81.6% in near-infrared region, and low surface roughness of 0.85 nm, which are useful properties for their potential applications in tandem solar cell and infrared technology.

Keywords: aluminum-doped ZnO (AZO), $Zr_{50}Cu_{50}$, thin film metallic glass, optoelectrical properties, morphology

PACS: 73.21.Ac, 42.70.-a, 68.55.-a

DOI: 10.1088/1674-1056/ab6c50

1. Introduction

Transparent conductive oxide (TCO) films have many electrical applications due to their high transparency and good electrical conductivity. Al-doped ZnO (AZO) has been developed as a promising material due to its low temperature growth, cheap cost, and environmental stability.^[1-4] Especially, the high infrared transmittance gives AZO broad application prospects in tandem solar cells and infrared technology. Since the optical and electrical properties of AZO films are still not sufficient to meet the requirements for high efficiency devices, much effort has been devoted to the development of AZO with low-resistive and high-transmittance. The thickness increment of AZO films could promote their electrical characteristics, but weaken the quality due to the enlargement of absorption coefficient and surface roughness. In particular, near-infrared transmittance declines sharply. In order to reduce the thickness of AZO, the buffer layer is introduced and the conductivity and transparency are both confirmed to be improved. Lots of buffer materials have been developed including ITO, ZnO, Al_2O_3 , MgO, ZnS, pure metal, and so on.^[5-10] Among them, the metal buffer can effectively raise the conductivity of AZO thin film. Nonetheless, it also causes the transmittance of

AZO/metal film to decrease since the continuous thin film can be formed only when the thickness of the metal films is over 10 nm. Recent investigations have reported that inserting thin film metallic glass (TFMG) between the substrate and TCOs presents both low resistivity and high transmittance. Lee *et al.*^[11] has reported the ITO/ZrCu bi-layer films with transmittance of 73% and sheet resistance of 20 Ω/\square . The ITO film with $Ag_{22}Al_{46}Mg_{32}$ as a buffer exhibits the visible transmittance of 80% and the sheet resistance of 15 Ω/\square .^[12] Lin *et al.*^[13] have found that AZO films shows the sheet resistance of 85 Ω/\square and the visible transmittance of 74% after inserting $Ag_{40}Mg_{40}Al_{20}$ TFMG as buffer.

Unlike traditional crystalline metals, metallic glasses (MGs) appear without dislocations or grain boundaries. TFMGs are expected to have distinctive electrical properties, *e.g.*, less electron scattering. Owing to its amorphous nature, TFMG possesses better surface roughness, and the optimal thickness of TFMG interlayer is lower than that of the conventional metal film.^[14,15] Moreover, TFMG exhibits extremely temperature sensitivity and unique characteristics in the supercooled liquid region (*i.e.*, ΔT , the temperature range between the glass transition temperature and the crystallization temperature). For example, Liu *et al.*^[16] found that the thermal

*Project supported by the National Natural Science Foundation of China (Grant No. 51571085), the Key Science and Technology Program of Henan Province, China (Grant No. 19212210210), the Foundation of Henan Educational Committee, China (Grant No. 13B430019), and the Henan Postdoctoral Science Foundation, China.

†Corresponding author. E-mail: haitaonzong@163.com

‡Corresponding author. E-mail: ghcao@hpu.edu.cn

stability for ZrCuNiAlHfTi TFMGs decreases with substrate temperature increasing. Chu *et al.* has reported^[17] that after annealing within ΔT , the $\text{Cu}_{51}\text{Zr}_{42}\text{Al}_4\text{Ti}_3$ film transforms from crystalline into amorphous structure and its surface becomes smooth. These factors would affect the properties of AZO with TFMGs as buffer. However, there are few reports about the influence of these factors on the structural and optoelectrical properties of AZO/TFMG bi-layer films.

Many deposition techniques have been used to prepare the AZO films including pulsed laser deposition (PLD),^[18] magnetron sputtering,^[19] chemical vapor deposition,^[20] sol-gel,^[21] and atomic layer deposition.^[22] Among these techniques, PLD technology is widely adopted because of good adhesion, strong controllability, and expected stoichiometric ratio. After decades of development, plenty of MGs have been presented such as Zr-based, Cu-based, Ni-based, Mg-based, *etc.*^[23–25] The $\text{Zr}_{50}\text{Cu}_{50}$ binary alloy is a promising material with simple composition, strong undercooling ability, high thermal stability, and unique solidification characteristics. In this work, AZO films each with $\text{Zr}_{50}\text{Cu}_{50}$ TFMG as buffer are prepared on the glass substrates by PLD. The effects of buffer thickness and substrate temperature on the properties of AZO thin films are systematically investigated by analyzing their structures, optoelectrical characteristics and morphologies, which reveals the possible mechanism behind the high transmittance and low resistance.

2. Experimental details

The AZO and $\text{Zr}_{50}\text{Cu}_{50}$ films were prepared on the glass substrates by PLD (COMPexPro 203) through using AZO ($\text{ZnO}:\text{Al}_2\text{O}_3$, 98:2 wt%) target and $\text{Zr}_{50}\text{Cu}_{50}$ (wt%) alloy target, respectively. The $\text{Zr}_{50}\text{Cu}_{50}$ (ZrCu) target was fabricated by arc melting high-purity metals of Zr and Cu together under Ti-gettered Ar atmosphere. In order to achieve chemical homogeneity, the ingots were melted four times, and then suction casted into copper mold with 20 mm×20 mm and thickness of 3 mm. The amorphous glass (BF33) is used as substrate, and its surface roughness is less than 1 nm. The films were deposited in a high vacuum (below 5×10^{-4} Pa), and the distance between the target and the substrate was maintained at 10 cm. The targets were ablated on the target surface using a KrF excimer laser at a pulse repetition rate of 5 Hz. The laser energy was 200 mJ. The target surface was ablated with a pulsed laser prior to film preparation to remove oxides and impurities. The samples with different thickness buffer were deposited at room temperature (25 °C). The thickness of AZO layer was fixed at 100 nm and that of ZrCu metallic films was varied from 4 nm to 20 nm. To evaluate the effects of the dependence of substrate temperature on the properties of films, AZO/ZrCu films were deposited at the temperatures of 120 °C, 200 °C, 280 °C, 360 °C, 440 °C, and 520 °C, respectively.

The thicknesses of AZO and ZrCu films were measured by α -step profilometer (DektakXT, Bruker), and the deposition rates were calculated. The structure of sample was characterized by x-ray diffraction (XRD, Rigaku D/MAX 200V/PC). The transmittance of thin film was probed by using an ultraviolet–visible–infrared (UV-3600, Shimadzu) spectrophotometer. The electrical performance was measured by using a Hall Effect system (HMS 5300, Ecopia). The surface morphology of the film was imaged by using an atomic force microscope (AFM, Dektak 150), and the roughness of film surface was calculated.

3. Results and discussion

3.1. Influence of ZrCu thickness

Figure 1 shows the XRD patterns of AZO films without and with ZrCu buffer layer for the case of different buffer thickness. As can be seen, single-layered AZO film has no characteristic diffraction peak, meaning that the AZO film deposited at room temperature possesses an amorphous structure. For none of all bi-layered films, diffraction peaks of ZrCu are observed, implying that the ZrCu layer has an amorphous structure. The AZO diffraction peak is detected for none of the films with small buffer thickness (4 nm and 8 nm), while a peak associated with the (100) AZO is found for each of the films with large buffer thickness (≥ 12 nm). The results reveal that inserting ZrCu buffer can promote the crystallization of AZO films. The large thickness of ZrCu buffer as sufficiently performing diffusion barrier could protect AZO material from being additionally oxidized, to achieve the thermal recrystallization of AZO. With the buffer thickness increasing, the (100) peak position shifts toward lower diffraction angles from 31.02° to 30.69° . The interplanar spacing (d) can be determined according to Bragg equation as follows:

$$2d \sin \theta = \lambda, \quad (1)$$

where λ is the x-ray wavelength and θ is the diffraction angle. As the thickness of ZrCu buffer layer increases from 12 nm to 20 nm, the deposition time increases and then the sample temperature increases. As a result, the subsequent deformation of cooling substrate occurs, which simultaneously induces the stress to change and eventually causes the d value of AZO film to rise.

There is no preferred growth of (002) crystal plane for any AZO bi-layer film in this experiment, which is obviously different from that for AZO film with other buffers existing at present (*e.g.*, Al_2O_3 and ITO).^[26,27] Generally, owing to the lower surface energy of (002) plane (9.9 eV/nm^2) than that of (100) plane (20.9 eV/nm^2), ZnO film grows preferentially in the (002) crystallographic direction. If ZnO is deposited under non-thermodynamic equilibrium conditions, it is possible to obtain other crystal planes. Growth of thin film at room

temperature by PLD is a typical non-thermodynamic equilibrium condition. Meanwhile, TFMG has a metastable structure. In the deposition process of AZO film on ZrCu layer, atomic clusters in TFMG obtain the energy and are rearranged gradually, resulting in the fact that the non-thermodynamic equilibrium condition is aggravated. The degree of influence increases with ZrCu thickness increasing. Therefore, uncommon (100) orientation is present and the (002)-oriented growth is hindered for samples with the buffer thickness between 12 nm and 20 nm.

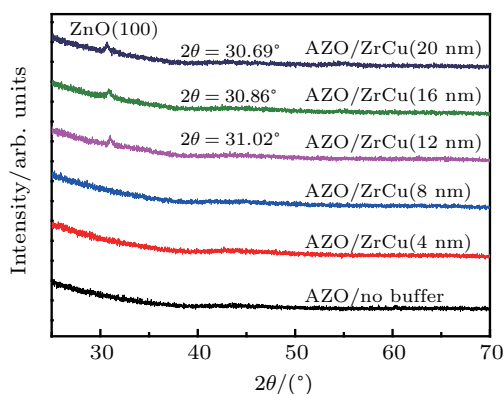


Fig. 1. XRD patterns of AZO films with different buffer thicknesses.

Table 1. Optical and electrical properties of AZO/ZrCu films with different buffer thicknesses.

Thickness of $Zr_{50}Cu_{50}/nm$	Transmittance		Sheet resistance $/(Ω/±0.2)$	Mobility $/(cm^2/V·s)$	Carrier concentration $/10^{21} cm^{-3}$	Figure of merit/ $10^{-3} Ω^{-1}$
	550 nm/%	1400 nm/%				
0	80.2	67.5	203.9	2.72	1.08	0.59
4	78.8	73.2	83.1	3.47	2.71	1.32
8	78.8	67.9	84.6	3.17	2.91	1.11
12	74.4	75.9	109.6	3.04	2.34	0.63
16	73.3	69.2	113.2	3.05	2.26	0.45
20	69.9	71.4	111.9	4.11	1.69	0.28

Figure 2(b) displays the variations in sheet resistance, carrier concentration and mobility of the AZO/ZrCu films with buffer thickness. It can be seen that the sheet resistance of all bi-layered film is lower than that of single-layered AZO film. After inserting a 4-nm ZrCu buffer, the sheet resistivity of AZO film varies from $203.9 Ω/□$ to $83.1 Ω/□$. Exactly, inserting the 4-nm ZrCu layer reduces about 145% resistance of the AZO film. With thickness of ZrCu layer increasing, the sheet resistance first increases and then stabilizes at the ZrCu thickness bigger than 12 nm. However, this result is contradictory to other reported results about TFMG serving as buffer. Lin and Chung^[13] reported that $Ag_{40}Mg_{40}Al_{20}$ deposited by co-sputtering with an elemental metal target as buffer has improved the conductivity of AZO film, and the resistance of AZO/ $Ag_{40}Mg_{40}Al_{20}$ decreases with buffer thickness increasing from 6 nm to 12 nm. Lee *et al.*^[11] prepared $Zr_{54}Cu_{46}$ films by co-sputtering with an elemental metal target and found that the resistance of ITO/ $Zr_{54}Cu_{46}$ decreases as the thickness of buffer increases. They explained these results

The optical transmittance spectra of AZO films varying with ZrCu thickness are shown in Fig. 2(a). The AZO/ZrCu bi-layered film exhibits a similar transparent trend to a single-layered AZO film in the measured spectrum. In the visible region (400 nm–800 nm), the transmittance gradually decreases with ZrCu layer thickness increasing due to the bigger reflectivity of the ZrCu layer. The transmittance of the single-layered AZO film accounts for 80.2% of the visible wavelength of 550 nm, while the transmittance of the AZO film with 4-nm ZrCu occupies 78.8% of 550-nm wavelength. When the buffer thickness increases up to 20 nm, the transmittance of AZO bi-layered film decreases to 69.9% of 550 nm. In the near-infrared region (NIR) (800 nm–1600 nm), the transmittance decreases with the wavelength of incident light increasing, while the single-layered AZO shows the biggest reduction. It is noted that the transmittance of AZO film increases from 67.5% to 73.2% at 1400 nm after inserting a 4-nm ZrCu layer. The transmittance values are read out and summarized in Table 1. The results suggest that inserting ZrCu layer between AZO and the glass substrate can improve the transmittance of film in the NIR, which is a promising method for improving infrared detectors and tandem solar cells.

with the parallel electrical resistance circuit model because the bottom TFMG has a lower electrical resistance than the upper TCO layer. In the present work, the $Zr_{50}Cu_{50}$ film with a thickness of 100 nm has a sheet resistance of $5 × 10^6 Ω/□$, which is far higher than AZO film. Furthermore, the resistivity of $Zr_{50}Cu_{50}$ film shows a size-dependent effect, and increases exponentially as the thickness of the film decreases.^[28] The conduction of MGs occurs via the relatively few extended-state electrons and is limited by a disorder induced scattering process. The fewer the extended-state electrons and the higher the disordered degree, the slower the electron flow is. In a Zr–Cu binary alloy, $Zr_{50}Cu_{50}$ MG possesses the excellent glass-forming ability and a higher disordered degree, which means that there are few free electrons and poor electron transport. For the AZO/ $Zr_{50}Cu_{50}$ bi-layer film, $Zr_{50}Cu_{50}$ cannot provide additional free electrons and better transport to AZO. The divergence from the other reports may be ascribed to the higher electrical resistance of $Zr_{50}Cu_{50}$ TFMG than that of AZO layer. After inserting the $Zr_{50}Cu_{50}$ layer between AZO

and glass substrate, the carrier concentration and mobility are both increased. The carrier concentration and mobility increase from $1.08 \times 10^{21} \text{ cm}^{-3}$ to $2.71 \times 10^{21} \text{ cm}^{-3}$ and from $2.72 \text{ cm}^2/\text{V}\cdot\text{s}$ to $3.47 \text{ cm}^2/\text{V}\cdot\text{s}$ after inserting the 4-nm buffer layer, respectively. These variations in both values might be related to the change of microstructure. Aluminum is an effective donor, which substitutes for zinc, thereby increasing the concentration of free carriers in ZnO. The introduction of buffer layer promotes the transformation of AZO from amorphous to crystalline structure as detected by XRD. The order degree in AZO film is increased and the defects are reduced, and then the effective quantity of Al in ZnO can be increased. As a result, the electrical properties are improved. With the increasing of ZrCu thickness, neither of the values changes much.

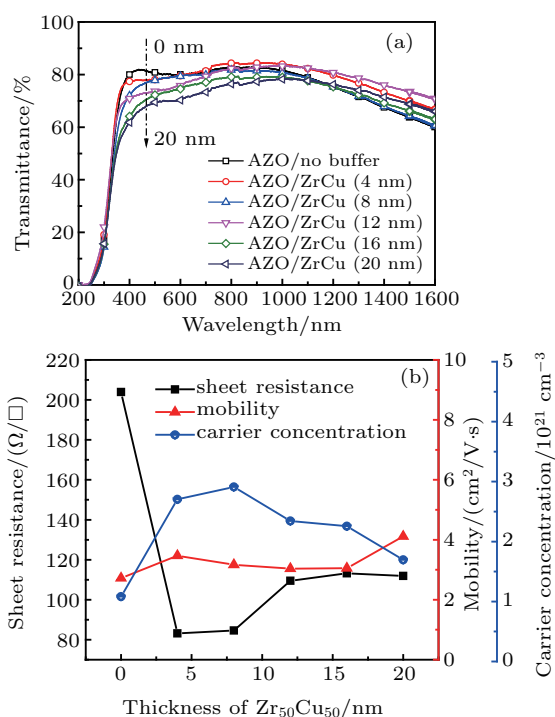


Fig. 2. (a) Optical transmittance spectra for various buffer thicknesses and (b) plots of sheet resistance, carrier concentration, and mobility versus ZrCu thickness of AZO/ZrCu films.

Figure 3 shows the AFM images of the AZO without and with the 4-nm ZrCu buffer. After inserting the ZrCu buffer, the root-mean-square (RMS) value of the films decreases from 2.61 nm to 1.09 nm, indicating the surface becomes smooth. The negative heat of mixing between Zr and Cu atoms ($-23 \text{ kJ}\cdot\text{mol}^{-1}$) will increase the attractive force during the deposition of ZrCu layer,^[29] and thus making the ZrCu layer a continuous and smooth film. The AZO film grown on the TFMG with smooth surfaces has better wettability than on the bare-glass substrate, and the defects in AZO film are reduced. As a result, the electrical properties are improved. In addition, an improved transmission in the NIR by introducing ZrCu buffer can be attributed to the increased carrier mobility.^[30]

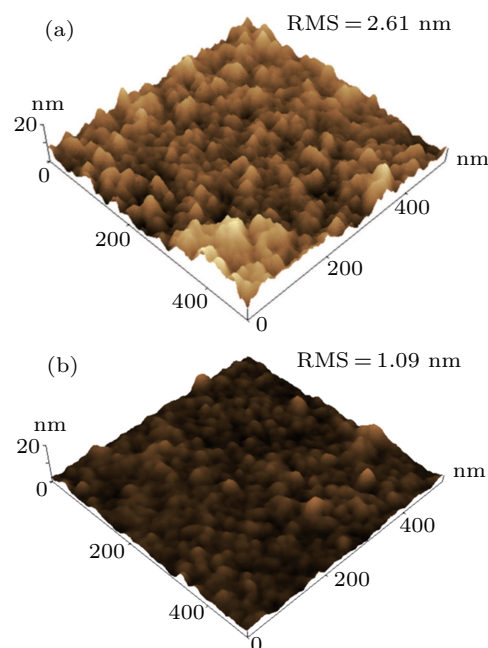


Fig. 3. AFM image of AZO film (a) without and (b) with 4-nm ZrCu buffer layer, respectively.

The basic requirement for a TCO film is that it should have high electrical conductivity combined with good optical transmittance. The quality of the film can be determined by a figure of merit (FOM) defined as^[31]

$$\text{FOM} = T^{10}/R, \quad (2)$$

where T is the average transmittance in a wavelength range of 400 nm–1600 nm and R is the sheet resistance. The higher FOM reveals the coincident high transmittance and low resistivity of thin film. The FOM values of the AZO/ZrCu films with different buffer thickness are calculated and also listed in Table 1. It can be found that the AZO film with 4-nm buffer evidently possesses the highest FOM ($1.32 \times 10^{-3} \Omega^{-1}$).

3.2. Influence of substrate temperature

In order to further improve the optical and electrical properties of the AZO/ZrCu films, the influence of the substrate temperature on the AZO/Zr₅₀Cu₅₀ film is investigated. The thickness of AZO layer and ZrCu are fixed at 100 nm and 4 nm, respectively. Figure 4 shows the diffraction patterns of the bi-layered films at different substrate temperatures. For none of all six films, diffraction peaks of ZrCu are observed, which suggests that the ZrCu layer retains the amorphous structure. It is seen that there is observed no AZO diffraction peak in the AZO thin film deposited at low temperature (120 °C), implying that thin films grown at low temperatures tend to form amorphous structures. For temperature higher than 200 °C, a prominent (002) reflection is detected at $2\theta = 34^\circ$. With the increase of substrate temperature, the intensity of diffraction peak gradually increases, and reaches a maximum value at 440 °C, and thereafter decreases. Increasing peak intensities implies the enhancement of the orientation

of the AZO grains. The crystallite size in the thin film (D) can be calculated from the Scherrer's formula

$$D = \frac{0.9\lambda}{\beta \cos \theta}, \quad (3)$$

where λ is the x-ray wavelength (1.523 Å) and β is the full width at half maximum (FWHM) of the Bragg angle θ . Based on Eq. (1), the value of D can be analyzed and summarized in Table 2. With the increasing of substrate temperature, D continuously increases and then decreases. The value of D is 8 nm for the film grown at low substrate temperature (200 °C), and increases to 26 nm for the film grown at high substrate temperature (440 °C), and then drops down to 22 nm for the film grown at 520 °C. The results reveal that increasing substrate

temperature can promote the crystallization of AZO films.

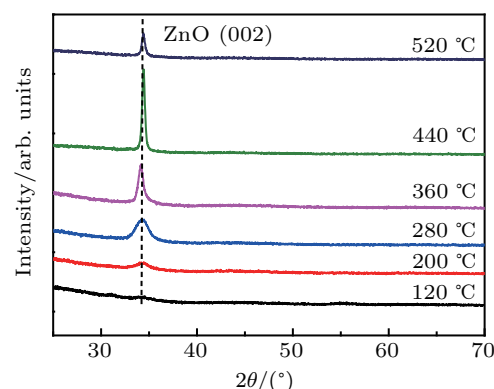


Fig. 4. X-ray diffraction patterns of AZO/ZrCu films deposited at different substrate temperatures.

Table 2. Optical, electrical, and morphological properties of AZO thin films with ZrCu buffer layer at different substrate temperatures.

Substrate temperature/°C	Average transmittance		Sheet resistance /($\Omega/\square \pm 0.2$)	Mobility /($\text{cm}^2/\text{V}\cdot\text{s}$)	Carrier concentration / 10^{20} cm^{-3}	Crystallite size/nm	Roughness /($\text{nm} \pm 0.05$)
	Visible light/($\% \pm 0.002$)	Near infrared/($\% \pm 0.002$)					
120	80.9	73.4	156.2	4.52	8.42	—	1.14
200	81.9	73.2	91.1	7.77	8.32	8.38	2.26
280	81.7	73.1	65.3	15.21	5.99	8.34	1.49
360	82.1	81.6	26.7	60.43	3.72	14.5	0.85
440	76.9	81.7	72.3	24.7	3.21	26.3	1.14
520	76.3	85.8	342.3	6.15	2.85	22.7	1.86

Figure 5(a) shows the transmittance curves of the AZO/ZrCu bi-layered films prepared at different substrate temperatures. In the visible region, all films are highly transparent and display an average optical transmission over 76%. With the increase of substrate temperature, the average transmittance first increases and then decreases, reaching a maximum of 82.1% at 360 °C. For the film deposited at high temperature, the crystallite size increases and the film becomes dense with less defects, resulting in the improvement of transmittance. But the further increase of the substrate temperature would make thin film worse, and then the light scattering is enhanced. In the NIR, the transmittance of film is sensitive to the substrate temperature. The transmittance of film grown at high substrate temperature is higher than at low substrate temperature. The average transmittance is about 73% at various temperatures in a temperature range of 120 °C–280 °C, increasing up to 81% at a temperature range of 360 °C–440 °C, and then increasing to 85% as the temperature further rising to 520 °C. The optical characteristics of AZO/ZrCu bi-layered films deposited at different substrate temperatures are listed in Table 2. The results indicate that appropriate substrate temperature can improve the optical transmittance of AZO/ZrCu film, especially in the NIR. It is worth noting that the infrared transmittance of AZO/ZrCu film deposited at 360 °C is 10.1% higher than that of the single-layered AZO film.

Figure 5(b) shows the plots of sheet resistance, mobility and carrier concentration versus wavelength of AZO/ZrCu

bi-layered film at different substrate temperatures. The electrical characteristics are also summarized in Table 2. With the increase of temperature, the sheet resistance first gradually decreases to a minimum value at 360 °C, and then rapidly increases. The minimum sheet resistance of the bi-layer film is approximately equal to 26.7 Ω/\square . With substrate temperature increasing, the Hall mobility of AZO/ZrCu film first increases and then decreases. When the substrate temperature increases from 120 °C to 360 °C, the mobility of AZO/ZrCu film increases from 4.52 $\text{cm}^2/\text{V}\cdot\text{s}$ to 60.43 $\text{cm}^2/\text{V}\cdot\text{s}$, about 12 times. The variation in the mobility might be related to the change of crystalline size with substrate temperature increasing as detected by XRD. The larger crystalline size reduces scattering at the grain boundary and increases carrier lifetime, so the mobility is increased.^[32,33] It is noted that the sheet resistance of bi-layered film deposited at 360 °C is 86.9% lower than that of the single-layered AZO film.

It is observed in Fig. 5(b) that the increase of the substrate temperature diminishes the free carrier concentration. The carrier concentration decreases from $2.72 \times 10^{21} \text{ cm}^{-3}$ of the film deposited at 25 °C to $2.85 \times 10^{20} \text{ cm}^{-3}$ at 520 °C (see Tables 1 and 2), which drops down an order of magnitude. According to the theory of semiconductor physics, the carrier concentration can be effectively increased by improving the crystallization quality. In the present work, the XRD results show that the increase of substrate temperature can improve AZO crystallization and promote grain growth, which causes the car-

rier concentration to be contrary to the experimental result. Therefore, it is reasonable to believe that the decrease of carrier concentration is not caused by the crystallization. On the other hand, the carrier concentration is directly related to the composition of the film. Lin *et al.*^[33] have found that the energy provided by high temperature could promote atom migration in AZO/Al₂O₃ bi-layered film, leading chemical composition of AZO layer to change. For the AZO/ZrCu system, the mixing heat values of Zr–Al, Zr–Zn, Cu–Al, Cu–Zn, and Zn–Al are –44 kJ/mol, –29 kJ/mol, –1 kJ/mol, +1 kJ/mol, and +1 kJ/mol, respectively.^[29] The Zr–Al and Zr–Zn have larger negative mixing heat and the ability to make atoms bonded strongly, which will increase the attraction between atoms. As is well known, aluminum as an effective donor can increase significantly the carrier concentration in ZnO film. For the AZO/ZrCu film, the atoms could obtain more energy to migrate on the surface of ZrCu in high temperature deposition process. Owing to the strong attraction between Zr and Al, Al atoms close to AZO/ZrCu interface are more likely to bind tightly with Zr atoms. The higher the temperature, the greater the effect is. Therefore, the effective quantity of Al in ZnO can decrease. As a result, the increase of the substrate temperature diminishes the free carrier concentration. The change of carrier concentration is consistent with the behavior of the transmittance in the NIR. The improved transmission can be explained by a decrease of the free carrier absorption and an increase of mobility.

To further reveal the evolution of structure in the deposition process, AFM analysis is performed. Figure 6 shows the AFM images of the AZO/ZrCu bi-layer films deposited at different substrate temperatures. The surface is not featureless and this surface roughness is thought to be caused by the columnar structure. Its RMS value increases from 1.14 nm at 120 °C to 2.26 nm at 200 °C as a result of grain growth or coalescence of metastable nanocrystallites. For the film deposited at 360 °C, the surface becomes smooth and the RMS value decreases to a minimum value of 0.85 nm. When the substrate temperature increases to 520 °C, the grains become larger and the surface roughness increases to 1.86 nm. The roughness values of the films are summarized in Table 2.

The microstructure of the film is closely related to the substrate temperature. MG is essentially “frozen liquid”, and to a large extent the amorphous solid inherits the structure from its original liquid metal. The faster the cooling rate, the larger the preservation of amorphous structure is. Therefore, the ZrCu film deposited at 120 °C is prone to holding amorphous structure, and the AZO film deposited thereon exhibits low roughness (see Fig. 6(a)). With the increase of substrate temperature, the atoms in ZrCu can obtain more energy to migrate during deposition, which reduces the disorder of ZrCu film and weakens the smoothness characteristic of the

amorphous film.^[16] As a result, the number of cylinders on the bi-layered film increases, and the RMS value increases (see Fig. 6(b)). When the substrate temperature is further increased, all atoms obtain more energy to migrate, and then the columnar structures are joined together as shown in Figs. 6(c) and 6(d). Therefore, the surface of the film becomes flat, and the samples growing at 360 °C are smoothest. When the temperature reaches 440 °C, due to further increasing the migration of the atoms, the atoms can diffuse to the lower energy position to nucleate and grow. In addition, the Zr₅₀Cu₅₀ layer can exhibit the fluid state at 440 °C (in ΔT of Zr₅₀Cu₅₀),^[34] and also promote the migrating of atoms in AZO. So the boundary becomes more clear (see Fig. 6(e)). When the temperature is 520 °C, the atoms in AZO with excessive energy are difficult to keep at their original positions. Therefore, they show random nucleation and growth, resulting in the poor crystallization of AZO film as shown in Fig. 6(f). The morphological characteristic of AZO/ZrCu bi-layered film is consistent with the analysis by XRD.

The FOM values of the bi-layered AZO(100 nm)/Zr₅₀Cu₅₀ (4 nm) films deposited at different substrate temperatures are shown in Fig. 7. It can be found that the film deposited at 360 °C evidently possesses the highest FOM value ($4.97 \times 10^{-3} \Omega^{-1}$) five times higher than the FOM value of the film deposited at room temperature. This bi-layered film has the best optical and electrical properties.

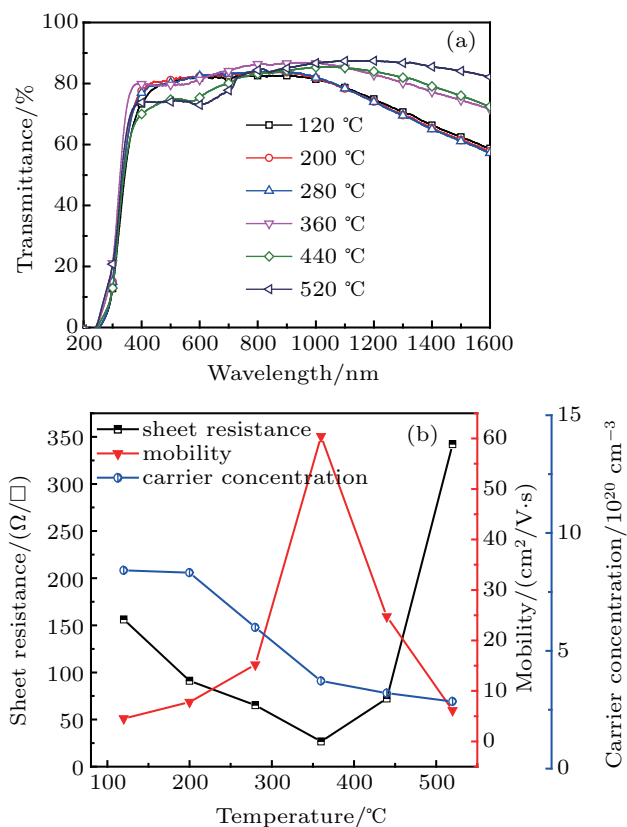


Fig. 5. (a) Optical transmittance spectra at different substrate temperatures and (b) plots of sheet resistance, carrier concentration, and mobility *versus* substrate temperature of AZO/ZrCu films.

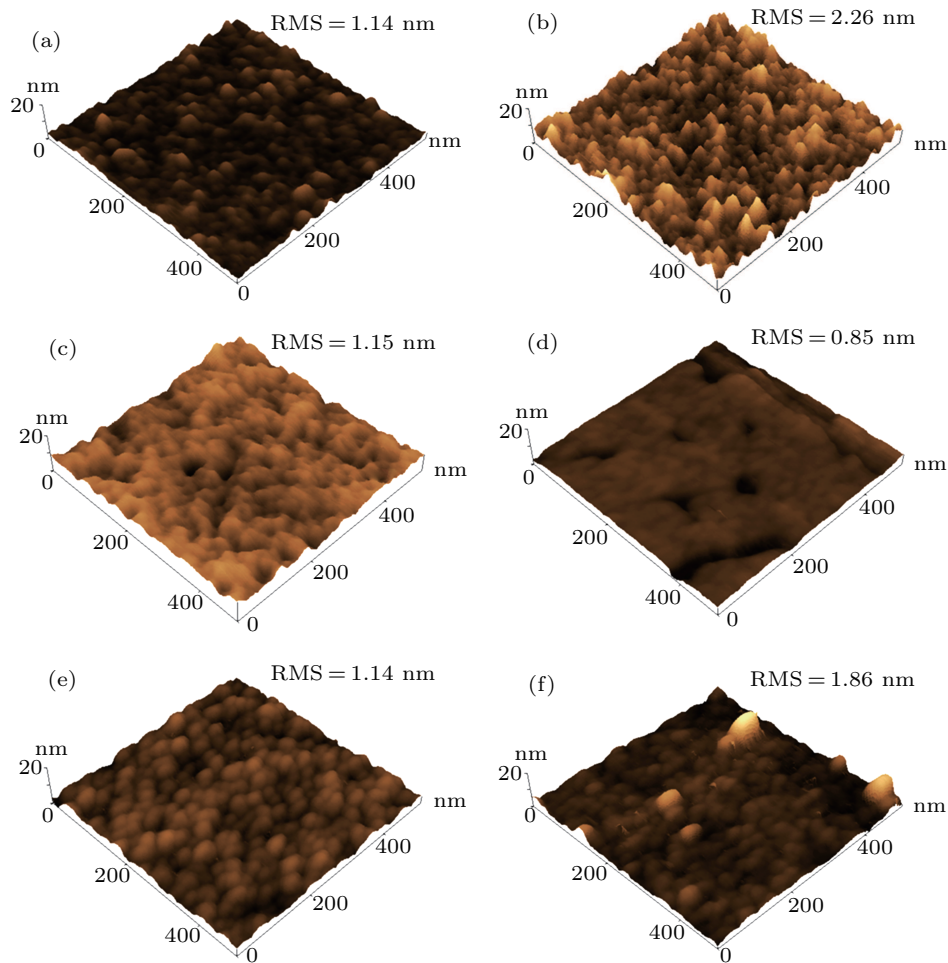


Fig. 6. AFM images of AZO/ZrCu films at different substrate temperatures: (a) 120 °C, (b) 200 °C, (c) 280 °C, (d) 360 °C, (e) 440 °C, and (f) 520 °C.

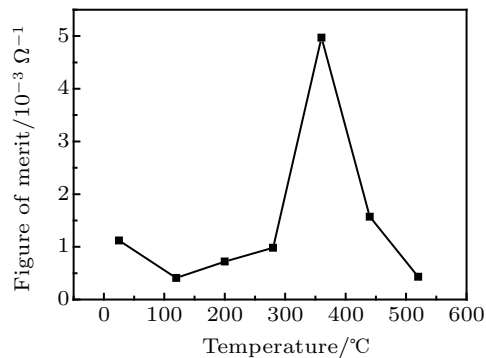


Fig. 7. Figure of merit for AZO/ZrCu varying with substrate temperatures.

4. Conclusions

The influence of $Zr_{50}Cu_{50}$ TFMGs as buffer layer on the structure, optical, and electrical properties of AZO films have been carefully investigated. As a result of inserting ZrCu film, the AZO/ZrCu bi-layered film is developed and exhibits the low resistance as well as high transmittance. The ZrCu thickness and substrate temperature can remarkably affect the structure of AZO film, and the single-oriented growth mode is observed. The AZO(100 nm)/ $Zr_{50}Cu_{50}$ (4 nm) film deposited at 360 °C shows the optimal properties, and possesses a sheet re-

sistance of $26.7 \Omega/\square$, average transmittance of 82.1% in the visible region and 81.6% in the NIR. Comparing with single-layered AZO film, the sheet resistance is reduced by 86.9% and the infrared transmittance is increased by 10.1%. The improvement of the properties is attributed to the smooth characteristic caused by ZrCu TFMG and the interaction between AZO and ZrCu. The electrical conductivity and the transmittance in the NIR of AZO by inserting ZrCu TFMG as buffer are strongly improved. This allows us to produce high-quality AZO thin film for transparent electrode applications in infrared techniques and solar cells.

References

- [1] Yang C W and Park J W 2010 *Surf. Coat. Technol.* **204** 2761
- [2] Shahid M U, Deen K M, Ahmad A, Akram M A, Aslam M and Akhtar W 2016 *Appl. Nanosci.* **6** 235
- [3] Ruske F, Pflug A, Sittinger V, Werner W, Szyszka B and Christie D J 2008 *Thin Solid Films* **516** 4472
- [4] Bamiduro O, Mustafa H, Mundle R, Konda R B and Pradhan A K 2007 *Appl. Phys. Lett.* **90** 252108
- [5] Rezaie M N, Manavizadeh N, Abadi E M, Nadimi E and Boroumand F A 2017 *Appl. Surf. Sci.* **392** 549
- [6] Babu BJ, Velumani S, Arenas-Alatorre J, Kassiba A, Chavez J, Park H, Hussain S Q, Yi J and Asomoza R 2015 *J. Elect. Mat.* **44** 699
- [7] Chen S J, Liu Y C, Ma J G, Lu Y M, Zhang J Y, Shen D Z and Fan X W 2003 *J. Cryst. Growth* **254** 86

- [8] Ashrafi A A, Ueta A, Kumano H and Suemune I 2000 *J. Cryst. Growth* **221** 435
- [9] Koike K, Komuro T, Ogata K, Sasa S, Inoue M and Yano M 2004 *Physica E* **21** 679
- [10] Crupi I, Boscarino S, Strano V, Mirabella S, Simone F and Terrasi A 2012 *Thin Solid Films* **520** 4432
- [11] Lee C J, Lin H K, Sun S Y and Huang J C 2010 *Appl. Surf. Sci.* **257** 239
- [12] Lin H K, Cheng K C and Huang J C 2015 *Nanoscale Res. Lett.* **10** 274
- [13] Lin H K and Chung B F 2019 *Appl. Surf. Sci.* **467–468** 249
- [14] Chu C W, Jason S C, Chen G J and Chiu S M 2008 *Surf. Coat. Technol.* **202** 5564
- [15] Lin Y T, Chung Y L, Wang Z K and Huang J C 2015 *Intermetallics* **57** 133
- [16] Liu S Y, Cao Q P, Qian X, Wang C, Wang X D, Zhang D X, Hu X L, Xu W, Ferry M and Jiang J Z 2015 *Thin Solid Films* **595** 17
- [17] Chu J P, Wang C Y, Chen L J and Chen Q 2011 *Surf. Coat. Technol.* **205** 2914
- [18] Coman T, Ursu E L, Nica V, Tiron V, Olaru M, Cotofana C, Dobromir M, Coroaba A, Dragos O G, Lupu N, Caltun O F and Ursu C 2014 *Thin Solid Films* **571** 198
- [19] Pat S, Mohammadigharehbagh R, Özen S, Şenay V, Yudar H H and Korkmaz S 2017 *Vacuum* **141** 210
- [20] Saini S, Mele P, Oyake T, Shiomi J, Niemelä J P, Karppinen M, Miyazaki K, Li C Y, Kawaharamura T, Ichinosef A and Molina-Lunag L 2019 *Thin Solid Films* **685** 180
- [21] Chen S, Warwick M E A and Binions R 2015 *Sol. Energy Mater. Sol. Cells* **137** 202
- [22] Banerjee P, Lee W J, Bae K R, Lee S B and Rubloff G W 2010 *J. Appl. Phys.* **108** 043504
- [23] Cao G H, Liu K, Liu G P, Zong H T, Balab H and Zhang B Q 2019 *J. Non-Cryst Solids* **513** 105
- [24] Yu Y Y, Xi F, Dai, C D, Cai L C, Tan Y, Li X M, Wu Q and Tan H 2015 *Chin. Phys. B* **24** 066201
- [25] Kyeong J S, Kim D H, Lee J I and Park E S 2012 *Intermetallics* **31** 9
- [26] Liu Y D, Wang X Y, Han Y and Chen H 2018 *Bull. Mater. Sci.* **41** 106
- [27] Rezaie M N, Manavizadeh N, Nadimi E and Boroumand F A 2017 *J. Mater. Sci.: Mater. Electron.* **28** 9328
- [28] Hu X X 2018 *The microstructure and optical and electrical properties of the Cu₅₀Zr₅₀ thin film metallic glasses* (MS Thesis) (Harbin: Harbin Institute of Technology) (in Chinese)
- [29] Takeuchi A and Inoue A 2005 *Mater. Trans.* **46** 2817
- [30] Nomoto J I, Oda J I, Miyata T and Minami T 2010 *Thin Solid Film* **519** 1587
- [31] Haacke G 1976 *J. Appl. Phys.* **47** 4086
- [32] Papadopoulou E L, Varda M, Kouroupis-Agalou K, Androulidaki M, Chikodze E, Galtier P, Huyberechts G and Aperathitis E 2008 *Thin Solid Film* **516** 8141
- [33] Lin C J, Li X Y and Xu C Y 2019 *J. Mater. Sci.: Mater. Electron.* **30** 721
- [34] Yu P, Bai H Y, Tang M B, Wang W L and Wang W H 2005 *Acta Phys. Sin.* **54** 3284 (in Chinese)